EIGHTEENTH EUROPEAN ROTORCRAFT FORUM

I - 06

Paper No 89

DEVELOPMENT OF ACTIVE CONTROL TECHNOLOGY IN THE ROTATING SYSTEM, FLIGHT TESTING AND THEORETICAL INVESTIGATIONS

D. Teves, V. KLöppel

EUROCOPTER Deutschland, München, Germany

P. Richter

HFW, Kassel, Germany

September 15 - 18, 1992

AVIGNON, FRANCE

ASSOCIATION AERONAUTIQUE AND ASTRONAUTIQUE DE FRANCE

DEVELOPMENT OF ACTIVE CONTROL TECHNOLOGY IN THE ROTATING SYSTEM, FLIGHT TESTING AND THEORETICAL INVESTIGATIONS

by

D. Teves, V. KLöppel

EUROCOPTER Deutschland, München, Germany

P. Richter

Henschel Flugzeug-Werke, Kassel, Germany

Abstract:

The extension of the conventional rotor control system to individual control of the single rotor blades (IBC) implements a vast potential of enhancing helicopter flight performance. In order to test this system, at ECD new flight tests on a BO105 equipped with IBC were performed.

The control system has been realized utilizing pitch link actuators, replacing the control rods in the rotating system between swashplate and rotor blades. This represents the first flying four-bladed helicopter with the blades individually controlled. In order to reduce the number of free control parameters the IBC technology was tested in harmonic mode.

Compared to former flight tests, reported in ERF 1990, the control authority has been increased in order to better address vibration and noise reduction effects. These effects are discussed in comparison with theoretical results.

To extend the application envelope of the IBC system, in cooperation with NASA Ames, full scale tests in the 40 by 80 ft NASA wind tunnel will be performed in the beginning of 1993. Objectives of these tests are, in addition to vibration and noise reduction, minimizing of required power and stall flutter suppression. The envisaged tests and the required hardware as well as first theoretical studies on the physical effects aimed at are described.

1. Introduction

Since the aeronautical potential of todays helicopters is not yet fully exploited efforts should be made to extend the flight envelope, and to increase reliability, riding comfort and public acceptance. In detail, problems of stall, noise, vibrations, aeromechanic/aeroelastic stability, and required power have to be tackled. A tool to efficiently address these problems is the Individual Blade Control (IBC) of the helicopter rotor, which allows for each rotor blade a control behaviour uncoupled from the other blades. In particular, control signals of any desired harmonic and non-harmonic characteristic can be introduced, limited only by the dynamic range of the control actuator applied.

In order to study this technique, a research programme was startet in 1989 between ECD and Henschel Flugzeug-Werke (HFW) (Ref. 1.1) representing the first IBC flight test of a four-bladed rotor. The programme is supported by the German Ministries of Research/Technology and Defence. In the past, two flight campaigns have been performed at ECD on a BO105 equipped with an IBC system developed by HFW. The near term goal of these activities was the system function test and the acquisition of know how about IBC technology and efficiency as a base of an application to future helicopters. In a first step, the influence of IBC on dynamic hub loads, cabin vibrations, control loads and noise was investigated.

In order to reduce the analytical effort, it appeared necessary to limit the number of the control degrees of freedom. Therefore only 2/rev, 3/rev, 4/rev, and 5/rev control inputs were applied. This allowed additionally to control the plausibility of the flight test results with the aid of existing wind tunnel tests on "Higher Harmonic Control" technique at least above 2/rev (Ref.'s 5.2, 8.1, 8.3).

For safety reasons, the control authority, the flight velocity, and the loading factor were limited during the flight tests. In order to no longer underlie these restrictions, in the beginning of 1993 full scale IBC tests with a BO105 rotor will take place in the NASA Ames 40 by 80 ft wind tunnel. The goal of these tests will be the improvement of the existing knowledge by adressing vibratory hub load rejection, stall delay, and noise reduction.

In contrary to these tests, which are open loop trials, in a following wind tunnel test and in further flight tests closed loop Individual Blade Control will be studied in order to capitalize on the technical potential of this novel control technology.

2. Targets of IBC Application

There exist mainly two targets for future IBC application, that is the extension of the flight envelope of the helicopter and the increase of its acceptance by passengers and by the society in general .

In detail, this may be accomplished by a reduction of:

- oscillatory hub loads and cabin vibrations,
- exterior noise,
- required power in the stall region, and
- flightmechanic and aeromechanic/aeroelastic instabilities.

The suppression of dynamic loads and vibrations is a typical "Higher Harmonic Control" (HHC) task which is here carried out by IBC. Since the reduction of oscillatory hub loads does not imply inherently a decrease of cabin vibrations a particular control law for the latter ones and a tradeoff between both goals might be required.

Exterior helicopter noise can be reduced particularly in descent and manoeuver flight, when inpulsive noise ("blade slap") due to blade vortex interaction (BVI) appears. In addition IBC may be applied in order to indirectly influence the noise of high speed flight by enabling lower blade tip speeds. In this case the stall onset of the retreating blade will be delayed by appropriate pitch angle laws.

A reduction of the required power is predicted for the area of stall occurrance i.e. for high loading factors and/or high advance ratios. The power saving is expected to be attained by avoidance of stall.

An example for the possible increase of the flight mechanical stability by IBC is the suppression of the helicopter's pitching up tendency at the stall boundary by flap stabilizing (Ref. 2.1). The aeromechanical stability can be improved by increasing the lead lag damping by a feed back of the blade lead lag rate signals (Ref. 2.2). Finally the running of helicopter rotors near or even beyond the stall boundary will require a distinct damping effort with respect to the blade's stall flutter behaviour.

3. Characteristics and Capability of the HFW IBC System

Henschel Flugzeug-Werke (HFW) have developed an Individual Blade Control System, whose most outstanding features are the servohydraulic actuators in the rotating system. This configuration eliminates the limitations of active control systems installed below the swashplate (HHC). The control system has been developed for BO105 flight tests and in similar version for planned full scale wind tunnel tests (see chapter 7). The HFW IBC system designed for the BO105 flight tests features as main components (Fig. 3.1):

- one actuator per blade (1),
- electric (2) and hydraulic (3) slipring between fixed and rotating system,
- power supply and duct of control signals through rotor mast and rotor head (4),
- hydraulic installation including central unit (5), regulation pumps (6), and oil cooler (12)
- digital controller (7) for generation of control inputs and system control, and
- control and survey elements as the control panel for input of control amplitudes and phases (8), indicator and control switch for pilot and co-pilot (9), as well as mechanical (10) and electric (11) "EMERGENCY OFF" by a bypass in the hydraulic system.

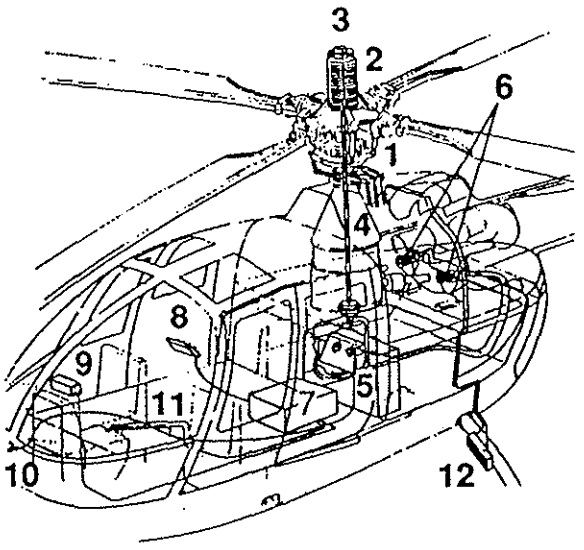

Fig. 3.1 IBC assembly in BO105

The actuators replace the conventional pitchlinks. They operate hydraulically and are controlled by servovalves. In case of hydraulic pressure loss the actuators are locked by springs in a definite position and act then like conventional pitchlinks. By this, collective and cyclic control is maintained in case of an IBC system malfunction. Fig. 3.2 illustrates the configuration for the full scale wind tunnel tests.

The IBC flight test system hydraulics is completely separated from the aircraft hydraulic system. Hydraulic power is generated by two pumps at the engines. After passing the hydraulic function box (central unit) with accumulators, valves, etc. it is fed through the rotor mast and head according to Fig. 3.1/3.3 (wind tunnel/flight tests). A hydraulic slipring and an electrical slipring transfer power and signals between the rotating and non-rotating frame.

The higher harmonic pitch angle and phase are generated by the operator ((8), Fig 3.1) and controlled by an internal IBC loop. The internal loop guarantees the identitiy of actual pitch angle and command input.

The internal IBC controller operates in its actual configuration in the frequency domain. The controller generates an individual signal for each actuator by a fourier synthesis of the con-

trol harmonics. The individual transfer behaviour of the servovalves etc. is compensated automatically.

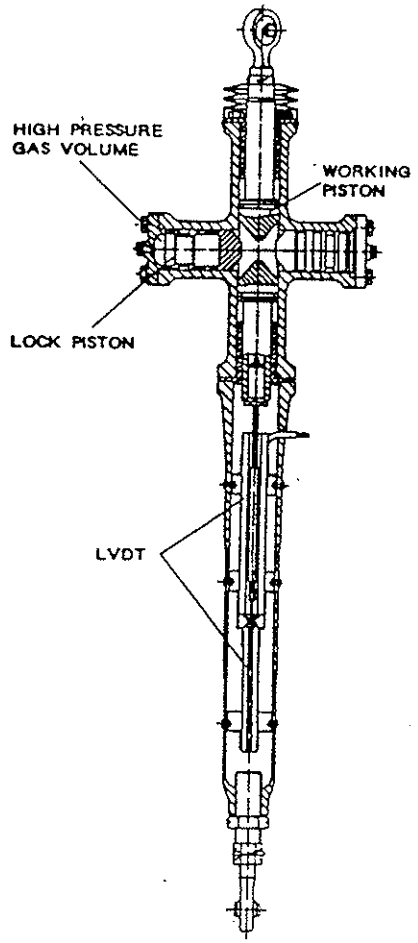

Fig. 3.2 IBC servo actuators replacing the pitch links

The HFW IBC system has several self-check features, including actuator stroke and force monitoring. If a load limit violation or malfunction is detected, the hydraulic supply is shunted. The resulting pressure drop activates the locking device of the actuators.

The performance data of the HFW IBC system are summarized in Table 3.1:

	flight test	wind tunnel test
actuator length	289 mm	682 mm
actuator stroke	± 1.5 mm	± 9 mm
IBC blade pitch	± 0.42°	± 3° (2/rev)
max. frequency	35 Hz	42 (64) Hz
hydr. pressure	207 bar	207 bar
actuator force	± 2000 N	± 5000 N
locking force min.	± 2000 N	± 5000 N
actuator mass	2.5 kg	5.0 kg

Table 3.1 IBC system performance data

Dimensions and mass of the wind tunnel test actuator, both significantly higher than for the flight test version, are caused by the specific model test rig configuration at NASA Ames.

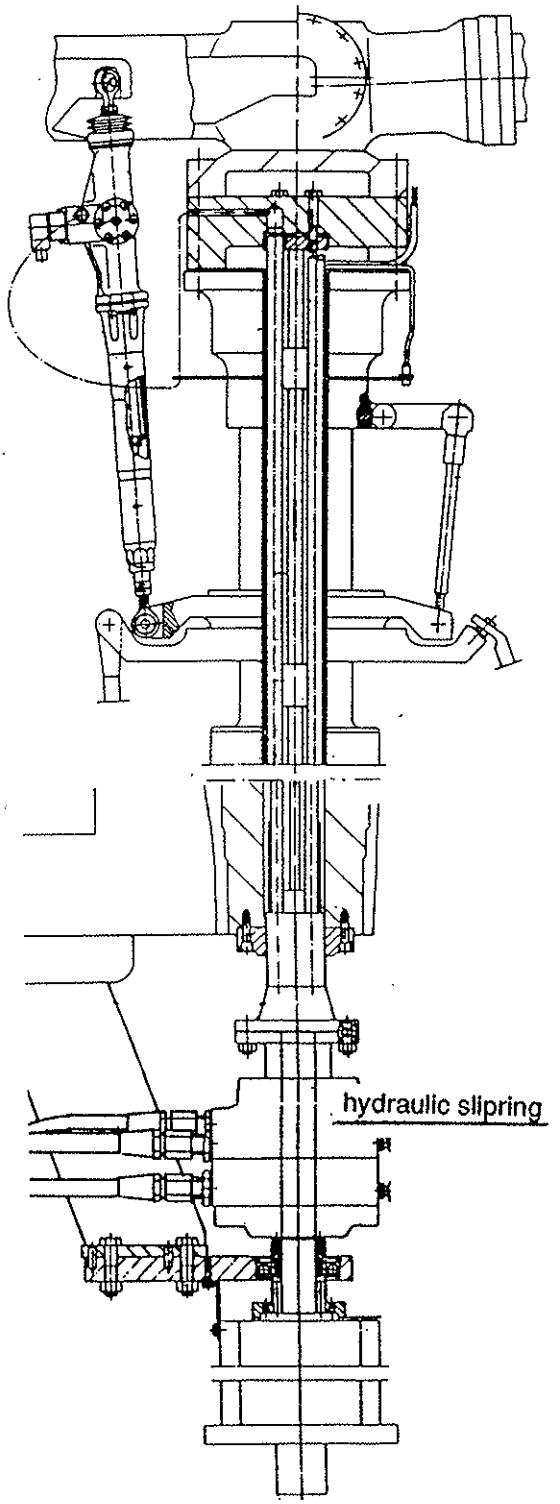

Fig. 3.3 IBC power supply through shaft and hub (WT configuration)

During the flight test, the IBC command input was performed by 9 potentiometers to accomplish the 2/rev, 3/ rev, 4/rev, and 5/rev amplitudes and phases. For the wind tunnel test, a PC-based input device is provided for easy test preparation and operation.

The IBC system for the wind tunnel test has a redundant stroke monitoring. Actuator travel versus commanded signal is monitored by two completely independent systems, each of them including a computer for fourier analysis and synthesis. If a malfunction is detected, or a difference between the systems occurs, hydraulic power is cut off. This feature makes an uncontrolled actuator travel virtually impossible.

The flight test actuators lock in their maximum diplacement (equivalent to minimum pitch) position, whereas the wind tunnel test actuators lock in their neutral position, in order to avoid large jumps of the collective pitch due to the large actuator stroke. For the flight tests, the control authority of the IBC actuators is therefore limited to $\Delta\theta = 0{,}42°$.

For the flight tests, the electric sliprings and the small, lightweight hydraulic slipring developed by HFW are located above the rotor. In the wind tunnel, the sliprings are located below the main gearbox of the test bed, and a standard hydraulic slipring is used.

All components as well as the complete system were tested thoroughly at the HFW facility in Kassel. This included functional tests, actuator fatigue life tests, a 400-h run on a main gearbox test stand and a whirl tower test at the ECD Ottobrunn facility. The tests showed a good system performance and proved the system's feasiblity for IBC research. The Wind Tunnel IBC-system is actually being tested.

4. Experimental and Theoretical Investigations of Vibration Reduction

Subject of this chapter is the change of hub loads and airframe-vibrations due to IBC pitch angle inputs. For steady flight conditions, only frequencies are present, which are multiples of the numbers of blades. Flight tests have shown that the 4/rev contribution is always dominating. Therefore the compensation of the 4/rev vibrations and hub loads are of primary interest.

As a first step, open loop flight tests are analysed. The compensation of the 4/rev harmonic of the airframe vibration requires a 3/rev, 4/rev and 5/rev pitch angle input, in order to control collective and cyclic rotor modes. During the flight tests, one of these 3 frequencies was selected for the IBC pitch angle input and the phase was varied from 0° to 360° with a step size of 36°.

The IBC pitch angle amplitudes were during the first test 0.16° and during the second 0.4°. The tests were performed for advance ratios of 0.14 and 0.27 and flight velocities of 61 kts and 113 kts respectively. The pressure altitude was 5000 ft.

Table 4.1 contents the system data of the test vehicle BO105

average take off mass	2200 kg
blade number	4
airfoil	NACA23012
angular rotor velocity	44.4 rad/s
rotor solidity σ	0.07
blade twist (linear)	8°

Table 4.1 Relevant system data of BO105

For all results presented, the azimuthal position Ψ of the reference blade is zero when this blade is pointing rearwards.

4.1Vibration Reduction

The first step in order to investigate the origin of the vibrations is the analysis of the hub loads and moments in the rotating frame. Therefore first, a comparison of measured and calculated hub loads is presented. Later on, the resulting cabin vibrations will be discussed. All calculations have been conducted with the helicopter analysis program CAMRAD/JA which is described comprehensively in Ref. 4.1.

Only the rotor degrees of freedom are used to model the mechanical system. For the lower advance ratio of 0.14 a free wake model is used, in order to take the effects of blade vortex interaction into account. For the higher advance ratio of 0.27 a prescribed wake model is used. As trim parameters, the measured values of flight attitude and hubmoments are used.

Figure 4.1 shows the measured and calculated change of the shaft bending moments due to IBC for 3/rev and 5rev IBC pitch angle inputs. Here only those load harmonics are shown, which are identical with the frequency of the IBC-actuation. Both, measurement and calculation show that for the test configuration applied the 5/rev IBC pitch angle input is much more efficient than the 3/rev input.

The amount of change in the shaft moments due to IBC control inputs is nearly the same in measurement and calculation. Only the predicted optimal control phases differ. Further investigations have shown that inertial forces due to hub vibrations which are not included in the analysis can explane some of these differences. Another source of the observed phase shifts is the yaw angle of the helicopter, which - in contradiction to experimental practice - is assumed to be zero in the analysis.

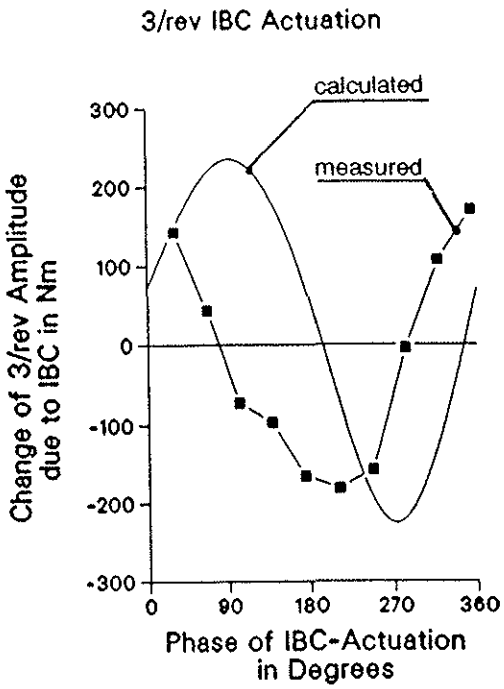

Flight speed (TAS) 61 kt

IBC amplitude 0.4°

Fig. 4.1. Change of shaft moment due to IBC (direct coupling)

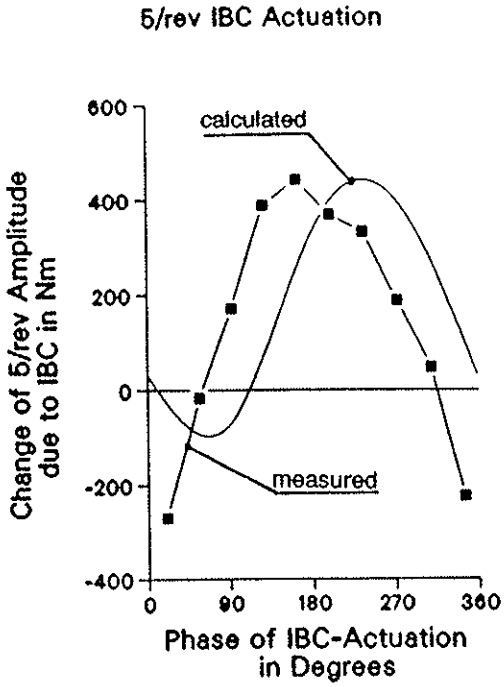

Fig. 4.1 Continued

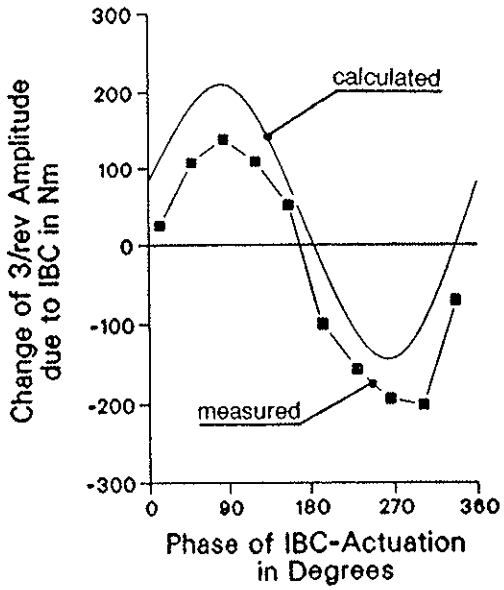

Flight speed (TAS) 61 kt

IBC amplitude 0.4°

Fig. 4.2 Change of shaft moment due to IBC (interharmonic coupling),

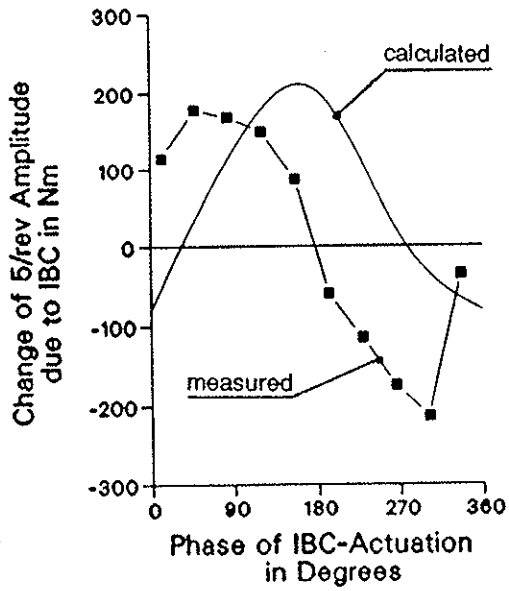

Fig. 4.2 Continued

Fig. 4.2 is similar to Fig. 4.1 with the exception that the frequency of the IBC actuation is not identical with the harmonic of the measured shaft bending moment. This transfer behaviour will be designated in the following text as "interharmonic coupling". Both, measurement and calculation show that the interharmonic couplings based on a 4/rev IBC pitch angle input cause nearly the same amount of change in the amplitudes of the shaft moment as the direct couplings shown in Fig. 4.1.

Fig. 4.3 shows the 3 components of the 4/rev cabine vibration for 3 IBC frequencies as a function of the phase of the IBC pitch angle. The figure demonstrates that especially the 5/rev IBC-input has a significant influence on the 3 components of the cabine acceleration. The optimal phases for each of the 3 components are different. Therefore, only by superposition of the 3 IBC frequencies an effective reduction of the cabine vibration levels may be achieved.

The highest amplitude change of the vertical cabin vibrations can again be attained by 5/rev control input. This excitation also has the largest effect on the 5/rev shaft bending moments shown in Fig. 4.2. The similarity of these two curves illustrates that the 5/rev shaft bending moment is most probably the dominant part of the excitation of the airframe in test configuration.

Since this dynamic characteristic doesn't harmonize with the excitation pattern of the serial BO105, it must be assumed that the big hub mass of the IBC-actuation system has changed the dynamic behaviour of the helicopter. This conclusion can also be drawn from the observation that even without IBC-control the vibrations of the test helicopter are lower than those of the serial version.

4.2 Transfer Behaviour

Subject of this chapter are the basic questions of the system identification. Most of the IBC-control algorithms are based on a linear transfer law in the frequency domain (Ref. 4.2) which is represented by the following equation:

$$\underline{y}_n = \underline{y}_{o_n} + \sum_{m=2}^{\infty} \underline{x}_{nm}$$

with $\underline{x}_{nm} = [T]_{nm} \cdot \underline{\Theta}_m \quad (4-1)$

and

$$\underline{y}_n = \begin{Bmatrix} y_{c,n} \\ y_{s,n} \end{Bmatrix} \qquad \Theta_m = \begin{Bmatrix} \Theta_{c,m} \\ \Theta_{s,m} \end{Bmatrix} \qquad y_{o_n} = \begin{Bmatrix} y_{oc,n} \\ y_{os,n} \end{Bmatrix}$$

$\underline{y}_{on}$ the n-th harmonic of a measured signal without IBC-input

$\underline{\theta}_m$ the m-th harmonic of the IBC pitch angle

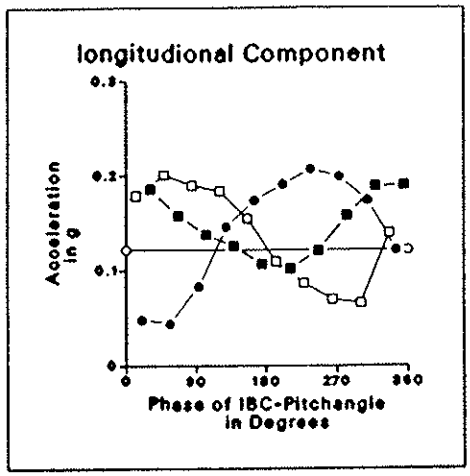

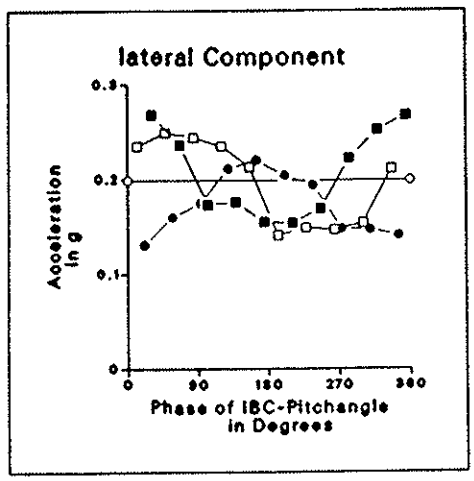

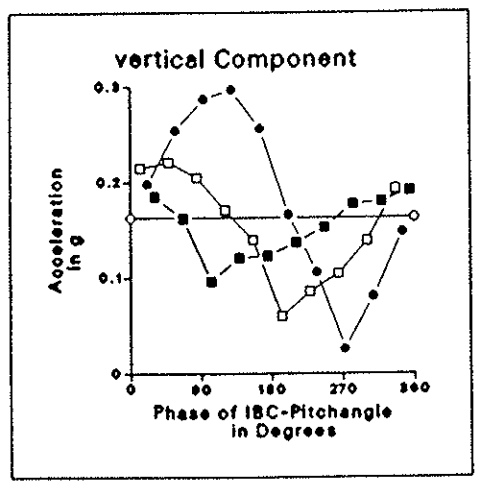

Frequency of IBC-Actuation in per rev

■ 3 □ 4 ● 5

○ **without IBC**

Harmonic	:	4/rev
Flightspeed TAS	:	61 Knots
Amplitude of IBC-Pitchangle	:	0.40 Degrees

Fig. 4.3 Reduction of cabin vibrations

$\underline{y}_n$ the n-th harmonic of a measured signal with IBC-input

$\underline{x}_{nm}$ the change of the n-th harmonic of a measured signal due to an m/rev IBC control input

The components of the vectors shown above are the sine and cosine coefficients of the fourier series representation

$$z(\psi) = z_o + \sum_{n=1}^{\infty} z_{c_n} \cdot \cos n\psi + z_{s_n} \cdot \sin n\psi \quad (4-2)$$

$$\text{so} \quad \underline{z}_n = \begin{Bmatrix} z_{cn} \\ z_{sn} \end{Bmatrix} \quad for \quad (\underline{z} = \underline{y},\ \underline{y}_o,\ \underline{\Theta},\ \underline{x})$$

The matrices $[T]_{nm}$ are submatrices of the T-matrix (Ref. 4.2).

Fig. 4.4 shows graphically the transfer behaviour of Equation (4-1). If the amplitude of the m/rev IBC-pitch angle Θ is constant and the phase is shifting, the resulting change of the measured n/rev signal $X_{n,m}$ generally describes an ellipse in the sin-versus cosine-coefficient plot. The ellipse is characterized by the axis lengths 2 a $\overline{\Theta}$, 2 b $\overline{\Theta}$ and the axis orientation angle α_E. The plot shows for four special ellipse points the corresponding phase values ψ_θ of the IBC pitch angle. An additional phase shift parameter $\Delta\psi$ indicates the position of the phase angle $\psi_\theta = 0°$ on the ellipse (see Fig. 4.5).

To sum up, the four parameters

a, b, α_E and $\Delta\psi$

are required in order to describe the transfer behaviour of the system. These parameters are related to the T-matrix of equation (4-1) by the expression.

$$\underline{T} = \underline{D}(-\alpha_E) \cdot \begin{bmatrix} b & 0 \\ 0 & a \end{bmatrix} \cdot \underline{D}(\alpha_E) \cdot \underline{D}(\Delta\psi) \quad (4-3)$$

$$\text{where} \quad \underline{D}(\gamma) = \begin{bmatrix} \cos\gamma & -\sin\gamma \\ \sin\gamma & \cos\gamma \end{bmatrix} \quad (\gamma = \alpha_E, \Delta\psi)$$

Fig. 4.5 depicts the corresponding measured transfer behaviour. The ellipses shown correspond to an IBC-pitch angle amplitude of $\theta = 0.4°$. The IBC phase is zero at the origin of the arrow and is increasing in direction of the arrows. The ten phase steps are marked by numbers of increasing sequential order. The reference point without IBC-Input is represented by the circle symbol.

Fig. 4.5 demonstrates that the ellipticity a/b characterizing the transfer behaviour strongly depends on flight speed. Tabl. 4.2 shows comprehensively the ellipse parameters discribing the change of the shaft moment as defined in Fig. 4.4. The corresponding T-matrix coefficients (Equation 4-3) can be used for a control design in the frequency domain in order to reduce the shaft moments. The parameters a and b describe the control efficiency. The highest values are always reached for the 5/rev shaft moments due to an 5/rev IBC input. High ellipticities of more than 2 exist only for the lower flight speed of 61 kts.

Flt spd	freq of IBC cont	harm of shaft mom	ellipse axis parameters		ellip-ticity	ellip. orien-tation	ph. diff
			a	b	a/b	α_E	$\Delta\psi$
kts	per rev		Nm/°	Nm/°		°	°
113	3	3	420	315	1.3	-38	131
		5	420	250	1.5	-63	157
	4	3	330	180	1.8	90	-165
		5	840	620	1.3	80	3
	5	3	370	280	1.3	70	-149
		5	1050	1050	1.0	79	- 42
61	3	3	630	255	2.5	-42	174
		5	645	150	4.3	-86	129
	4	3	480	330	1.45	-63	78
		5	495	355	1.4	86	-130
	5	3	375	287	1.3	78	-58
		5	1225	877	1.4	90	-45

Table 4.2: Ellipse parameters describing the change of the shaftmoment due to IBC-control
Amplitude of the IBC Pitch angle: 0.4°

5. Noise Reduction

As mentioned in chapter 2, the component of helicopter noise which can be influenced with best efficiency by IBC, is the impulsive noise by "Blade Vortex Interaction" (BVI) during descent and manoeuver flight. The mechanism to which the beneficial impact of IBC may be attributed is actually seen in:

- an increase of the misdistance between blade tip vortices and blade interfering with these or
- a reduction of the compressiblity effects caused by the blade vortex interaction by lowering the blade pitch angle during the intersection instant. (Ref.'s 5.1, 5.3)

Both targets can be attained already with good success by Higher Harmonic Control by applying 3/rev, 4/rev and 5/rev control or an appropriate combination (Ref.'s 5.1, 5.2).

relation between input and output signal:

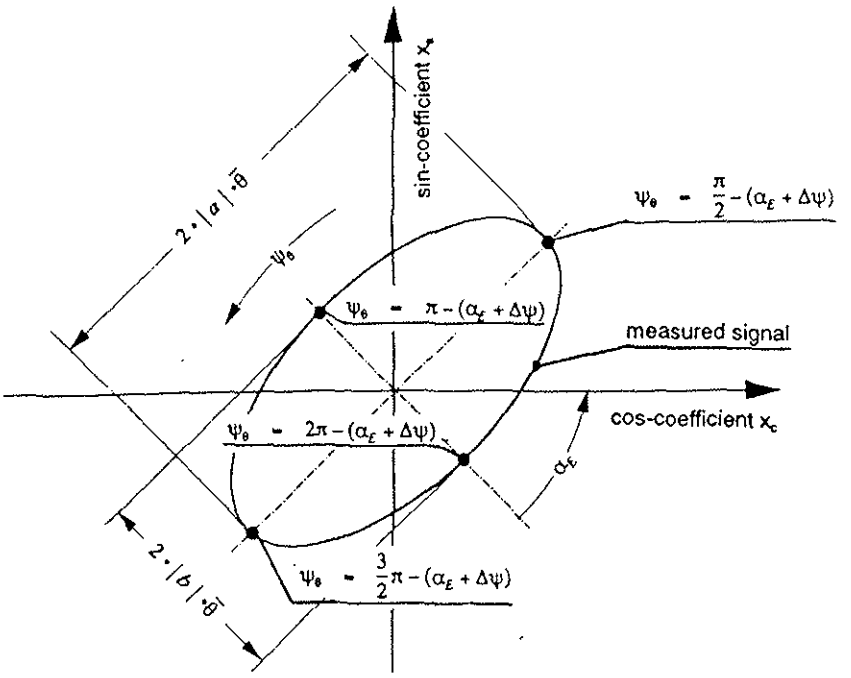

$$\begin{Bmatrix} x_c \\ x_s \end{Bmatrix}_n = [T]_{nm} \cdot \begin{Bmatrix} \theta_c \\ \theta_s \end{Bmatrix}_m$$

$$[T]_{nm} = [T(a, b, \alpha_E, \Delta\psi)]_{nm}$$

input signal: $\theta_m(\psi) = \theta_c \cdot \cos(m \cdot \psi) + \theta_s \cdot \sin(m \cdot \psi) = \bar{\theta} \cdot \cos(m \cdot \psi - \psi_\theta)$

output signal: $x_n(\psi) = x_c \cdot \cos(n \cdot \psi) + x_s \cdot \sin(n \cdot \psi)$

Fig. 4.4 Transfer behaviour of IBC input and system response

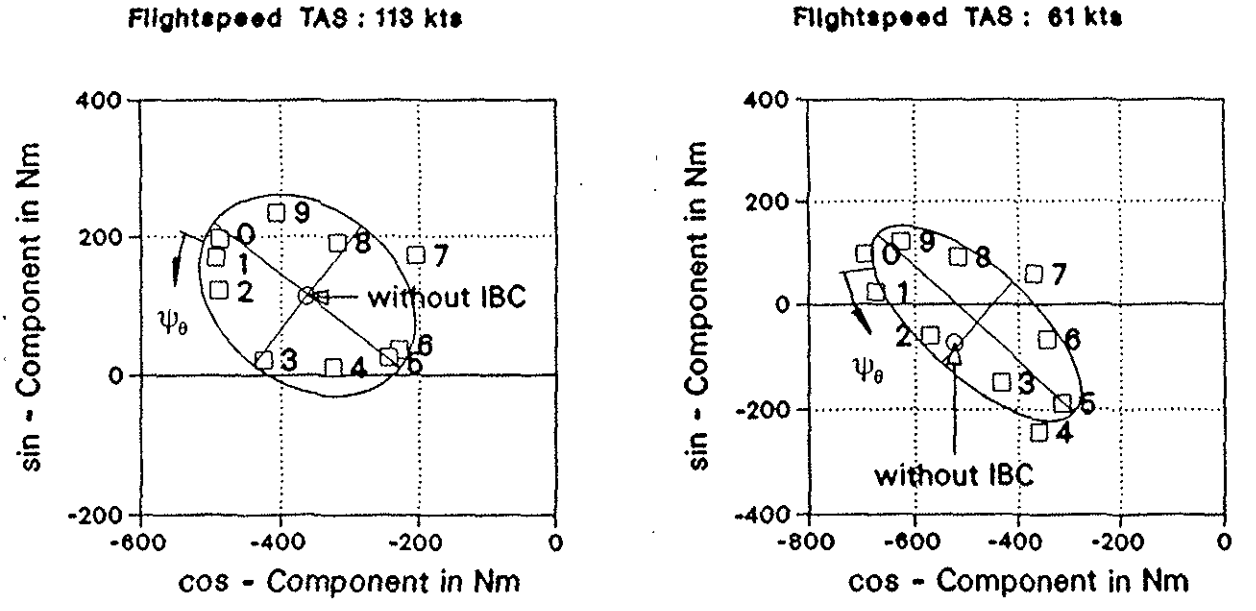

Frequency of the IBC Pitchangle: 3/rev
Amplitude of the IBC Pitchangle: 0.4 Degrees
Phase of the IBC Pitchangle: $\psi_\theta = n_\theta \cdot 36° - 5°$ $(n_\theta = 0,1....9)$

Fig. 4.5 3/rev shaft bending moment

Since the duration of the BVI event is short and a sometimes unfavourable side effect on vibratory rotor loads has been observed, a minimization of the noise reducing control signal in form of a wavelet, i.e. a short up/down or down/up pitching appears desirable. The generation of a steep wavelet and particularly of several wavelets during one rotation for the compensation of different BVI events can be duely performed by superposition of higher pitch harmonics by IBC.

Since actual tests with IBC are still in a phase of basic exploration, the flight tests aiming at noise reduction were performed by applying only a 5/rev control. This allowed to profit from wind tunnel tests in the DNW with a BO105 model rotor (Ref 5.2). During the flight tests, the helicopter, a BO105, performed a descent flight with a velocity of v = 65 kt and a glide path angle $\psi = 6°$ over a ground microphone. The noise radiation time history is presented in Fig. 5.1. As the BVI noise on the advancing blade side is radiated mainly forward the noise reduction occurs during the approach phase.

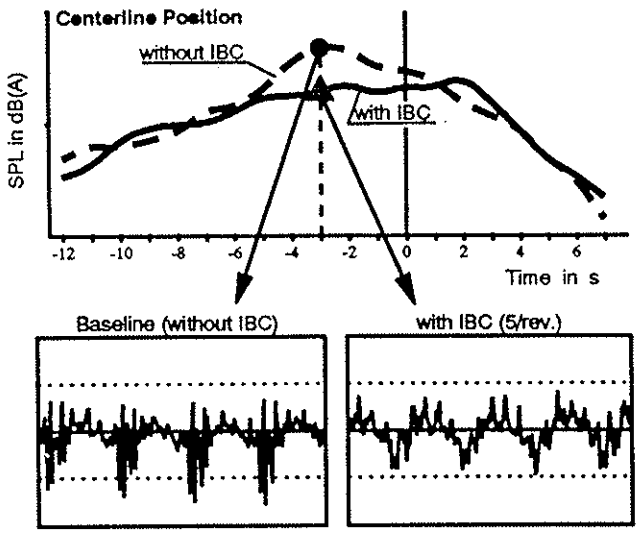

Fig. 5.1 Fly over noise time history of BO105 with and without 5/rev control

The successful reduction of noise impulsiveness can be seen from the significant change in the signal pattern of the noise power spectrum without and with IBC.

As indicated above, the flight test represented a replication of an HHC test with a BO105 model rotor (diameter d = 4 m) in the DNW. The correspondance of the noise results of both tests are illustrated in Fig. 5.2. In order to enable this comparison, the wind tunnel noise data acquired by a moving microphone array below the rotor had to be extrapolated from the measurement area to the scaled observer distance.

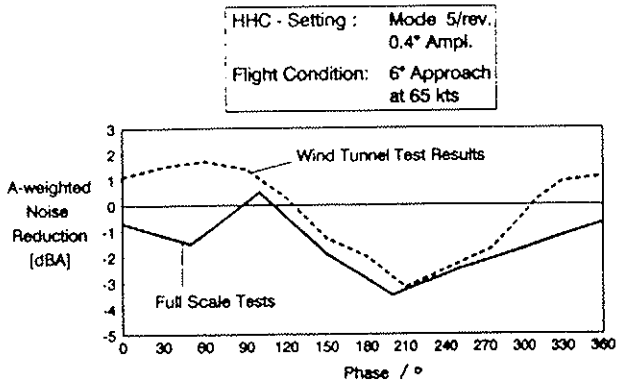

Fig. 5.2 Noise reduction comparison of full scale flight tests with wind tunnel tests for 5/rev control

6. Theoretical Evaluation of Power Reduction by 2/rev IBC

By application of the rotor analysis program CAMRAD/JA, the potential of IBC-technology to reduce the required power at the high μ/high g boundary of the helicopter flight envelope is investigated. The rotor considered is a BO105 rotor in high velocity cruise flight at $\mu = 0.426$. It should be noted that the computations are to give a phenomenological insight into the aerodynamics of extreme flight conditions and do not consider BO105 power restrictions. For the BO105, such advance ratios are only attainable in descent flight (Ref. 6.1).

For the analytical representation of the rotor, only a simple structural model of the rotor including the fundamental flap and lag modes is used. The propulsive force of the rotor is trimmed to a fixed value $C_H/\sigma = -0.0137$, which corresponds to a drag area of $D/q = 0.66\ m^2$. The hubmoments were trimmed to zero. A self-tuning control procedure is used in order to find the optimal combination of primary controls and IBC control inputs. A simple dynamic stall model based on Mach number dependent time delay constants is used. The inflow is modeled by trapezoidal velocity distribution.

The results depicted in Fig. 6.1 indicate the capability of IBC to increase maximum thrust at constant power and vice versa (see also Ref 6.2). The spreading of the curves for profile power promises further benefits at higher power and thrust levels, which however are not realistic for the rotor type considered. Since the attained benefits result from stall delay, power savings at increased maximum thrust are also expected for lower advance ratios.

In addition to stall delay efforts, it appears necessary for the envisaged high thrust regions comprising stall conditions to apply also stall flutter suppression by using active control technologies.

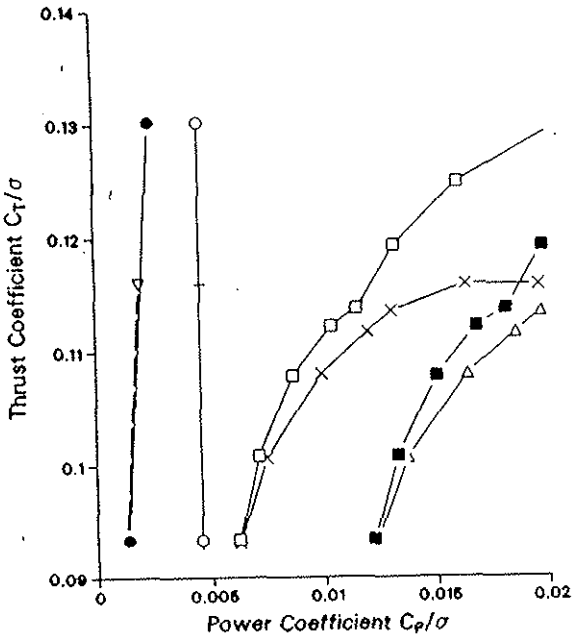

with IBC	without IBC
■ Total	△ Total
□ Profile	× Profile
● Induced	▽ Induced
○ Propulsive	+ Propulsive

Advance Ratio	:	0.426
mean Tip-Machnumber	:	0.65
Trimprocedure	:	Zero Hubmoment
Rotor Drag C_H/σ	:	-0.0137
Dynamic Model	:	2 blade bending modes
Inflow Model	:	trapezoid Inflow
Stall Model	:	$\sqrt{\zeta_\alpha}$ Stall Delay

Fig. 6.1 IBC impact on thrust/power characteristics under extreme flight conditions

Fig. 6.2 shows the trim and control parameters corresponding to Fig. 6.1.

7. Planned NASA Ames Wind Tunnel Test

IBC is one of several subjects in a joint US/German rotorcraft research effort. In January 1993, a full scale BO105 rotor equipped with the HFW IBC-system will be tested in the 40 x 80 ft wind tunnel at NASA Ames (see chapter 3 and Fig.'s 3.2 and 3.3) . The main objectives of the open-loop test, scheduled for 6 weeks of test time, are the identification of

- the system's operation characteristics,
- rotor reactions on single frequency IBC inputs to determine a T-matrix,
- attainable reductions of dynamic hub loads,
- effects of 2/rev control plus higher harmonics on flight envelope extension and power saving,
- methods of flap stabilization at the stall boundary,
- achievable reductions of blade vortex interaction noise,
- combinations of benefits and/or tradeoff effects concerning different application goals,
- baseline data for IBC controller design, and
- necessary improvements of theoretical models

8. Envisaged Feedback Systems

As can be seen from the preceeding chapters the Individual Blade Control features a system of pronounced complexity. So the system implies a high degree of freedom and requires a tradeoff between different control goals or a prioritization and harmonization of the goals if these are to be attained at the same time. Therefore a closed loop system appears mandatory (see Fig 8.1). Since particularly the second pitch harmonic may lead to a detrimming of the rotor nearly all methods will require a specific trim compensation loop.

For the control of vibratory loads at rotor hub (Ref. 8.1) and cabin (Ref. 8.2) closed loop systems have been proposed and partially tested. As suitable time domain method, the incorporation of 3/rev, 4/rev and 5/rev notch filters in the rotating system for dynamic blade root bending moments and shear loads is considered.

The closed loop exterior noise reduction under BVI conditions has been tested in the frequency domain (Ref. 8.3). A time domain feed back control will lead to significant acceleration of the controller response. The control signals will be provided either by microphones on the fuselage or pressure gauges on the blades. In case of a Blade Vortex Interaction these signals will generate a blade pitch wavelet of prescribed shape. Only phase and amplitude will be adapted in a way as to minimize the nose creating effect of further blade vortex interactions. In order to prevent undesired impacts on dynamic hub loads, the harmonics applied could be restricted to reactionless forms (2/rev, 6/rev, 10/rev,...).

In the case of stall delay efforts aiming at an increase of maximum thrust and power savings, a partially prescribed pitch angle curve, retaining the blade pitch along the azimuth just below the stall boundary, is envisaged, particularly by higher loading of the fore and aft sections of the rotor disc.

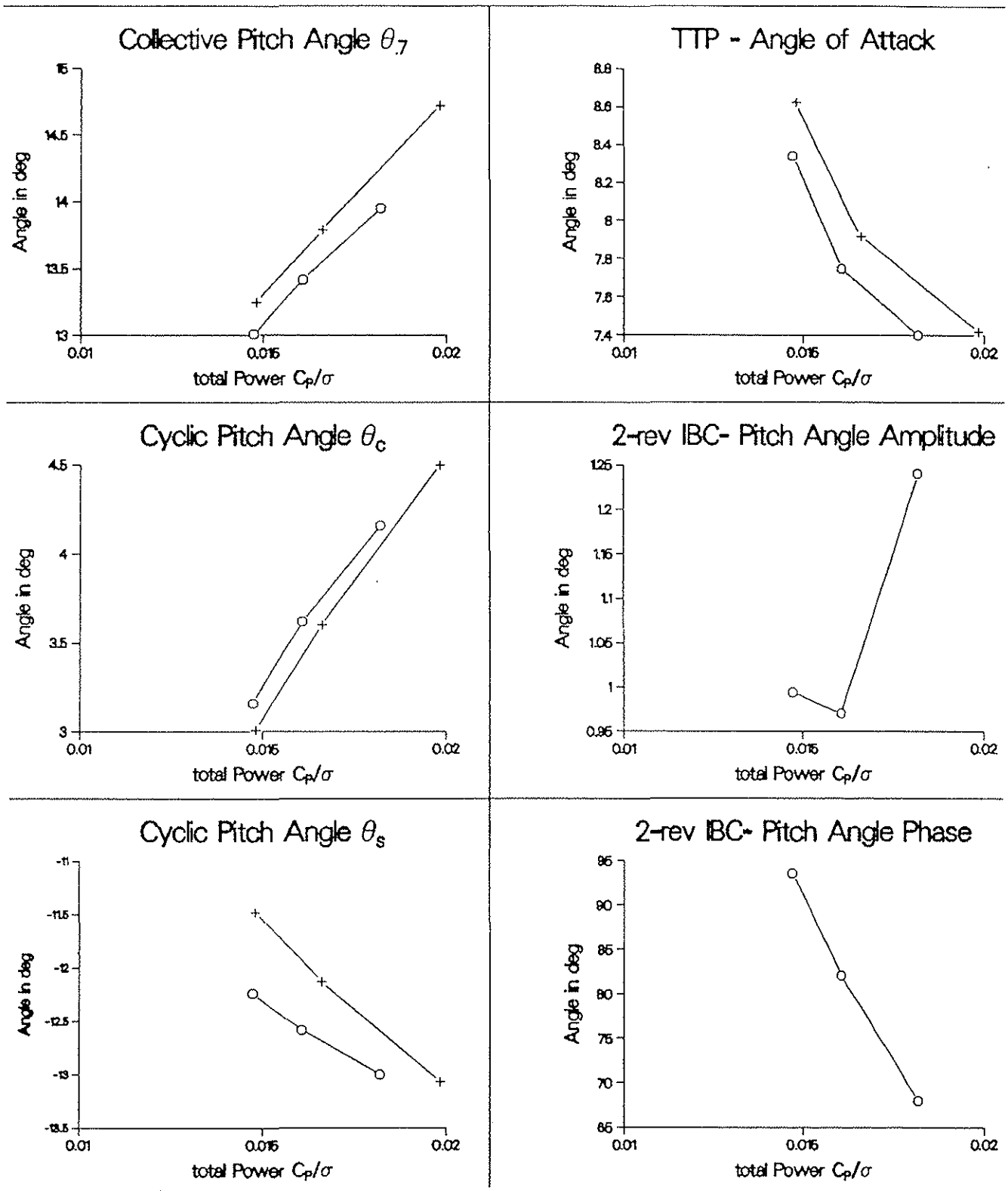

Fig. 6.2 Trim and control values for 2/rev input optimized for power reduction

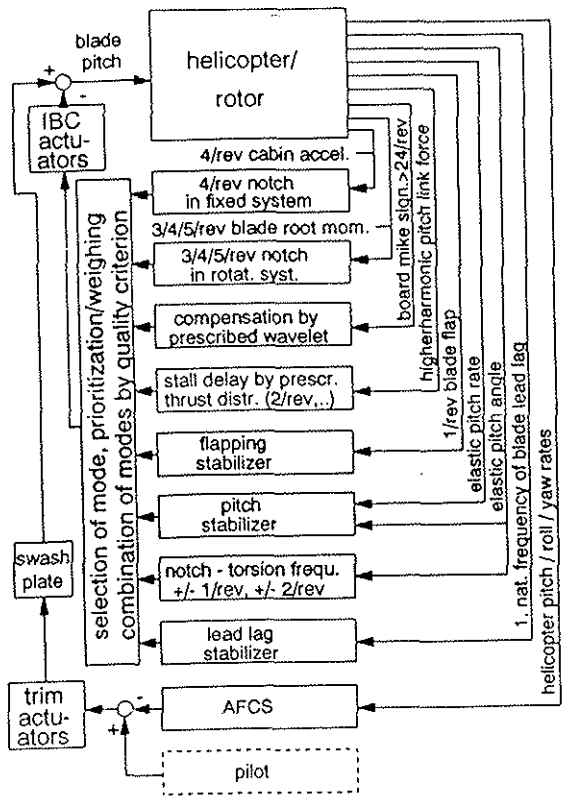

Fig. 8.1 IBC closed loop system for alternative or parallel application of different control tasks

The pitch curve will be composed by the second and higher harmonics which will be controlled by the feed back signal of blade pitch link forces or blade pressure transducers for stall identification.

Also the stabilizing of the rotor flapping at high speeds will take advantage from the stronger loading of the aerodynamically sound rotor disc segments. Hereby the local pitching down of the advancing blade will be compensated which is needed to suppress the flapping up of the rotor in the forward azimuthal position at beginning retreating blade stall (Ref. 2.1).

Inspite of the aforementioned activities to delay stall onset or to compensate its effects, stall flutter suppression particularly at high cruise speeds will be indispensable. It can be achieved by applying notch filters adapted to the first natural blade torsion frequency $\omega_{\theta B} + / - \Omega, 2\Omega, \ldots$ (Ref. 1.1). Herein Ω is the angular frequency of the rotor. In addition, the torsional blade motion will be stabilized by feed back of elastic pitch angle and pitch rate.

The damping of the lead lag mode of the rotor blades is achievable by a feed back of the blade's lag rate. The latter is to be integrated from signals stemming from accelerometers mounted on the blades (Ref. 2.2).

The large number of control tasks will require considerable efforts to either select the control mode most appropriate for an actual flight condition or to combine different tasks e. g. by a criterion of control effectiveness. So in case of high speed or high load factor flight conditions, noise and cabin vibration reduction could be defered. On the other hand, Ref. 8.3 demonstrates that compromises in the reduction of noise and vibratory rotor hub loads are possible.

9. Planned Continuation of IBC Technology Development

Todays expectations regarding IBC efficiency are based on theoretical calculations and limited flight tests. As a result, the opinions on IBC benefits are very different in rotorcraft community. The planned wind tunnel test at NASA Ames as well as future flight tests envisaged for closed loop trials are expected to give first answers to the following crucial questions for future IBC applications:

- What actuator stroke and force is required to achieve substantial benefits by IBC?
- What kind of controller concept is needed for closed-loop IBC operation?
- What will be the weight and cost penalty of an IBC system, and what kind of helicotper should be equipped with such a system?

With the know-how of the above tests it should be possible:

- to lay out feed back systems for the different application goals including consideration of their mutual compatibility,
- to test the most promising ones of these closed loop systems in the 40 x 80 ft NASA Ames wind tunnel, and
- to develop and establish a redundant and efficient control system for airborne application.

It is expected that these efforts will lead to the application of IBC in future advanced technology helicopters.

10.Conclusions

The first flight tests of a four bladed rotor controlled by an IBC system have taken place. On this occasion, a new control technology developed by Henschel Flugzeug-Werke in cooperation with ECD was tested on an ECD BO105. Though, mainly for simplicity reasons, only 2/rev, 3/rev, 4/rev and 5/rev were applied, an encouraging insight into the technical potential of this novel control technology was achieved.

The results show that the transfer behaviour of the hub loads due to the IBC actuation is well represented by the T-matrix approach. Theoretical investigations reveal, that the change of hub loads due to IBC can be predicted satisfactorily by an analytical isolated rotor model. With the current limitation of the maximum IBC pitch angle to 0.4° a complete cancellation of the hub moments cannot be achieved. In spite of this, remarkable reductions of the vertical cabine vibrations are observed.

By an optimal 5/rev IBC-actuation a remarkable reduction of the fly over noise level is obtained.

Analytical investigations show, that the flight envelope can be extended by the use of IBC especially for high thrust coefficients and high advance ratios.

In addition, it is expected that IBC will be a powerful tool in the area of stall flutter suppression and lead lag damping.

In general IBC will help to extend future helicopters' flight envelope and agility and will increase stability, riding comfort and public acceptance.

11.References

1.1 P. Richter, H.D. Eisbrecher, V. Klöppel, Design and First Tests of Individual Blade Control Actuators, 16th ERF, Paper No. 6.3, Glasgow, Sept. 1990

2.1 M. Kretz, Active Expansion of Helicopter Flight Envelope, 15th ERF, Paper No. 53, Sept. 1989

2.2 N. D. Ham, Research on Measurement and Control of Helicopter Rotor Response Using Blade-Mounted Accelerometers. 17th ERF, Berlin 1991

5.1 W. Splettstößer, G. Lehmann, B. van der Wall, Initial Results of a Model Rotor Higher Harmonic Control (HHC) Wind Tunnel Experiment on BVI Impulsive Noise Reduction, 15th ERF, Paper No. 1, Sept. 1989

5.2 T.F. Brooks, E.R. Booth, Rotor Blade-Vortex Interaction Noise Reduction and Vibration Using Higher Harmonic Control, 16th ERF, Paper No. 9.3, Sept. 1990

5.3 M. Lowson, Progress Towards Quieter Civil Helicopters, 17th ERF, Berlin, 1991

4.1 W. Johnson, Development of a Comprehensive Analysis for Rotorcraft I, II, Vertica, Vol. 5, 1981

4.2 W. Johnson, Self-Tuning Regulators for Multicyclic Control of Helicopter Vibations, NASA TP-1996, March 1982

6.1 H. Huber, H. Strehlow, Hingeless Rotor Dynamics in High Speed Flight, Vertica, 1976, pp. 39 - 53

6.2 M. Polychroniadis, Generalized Higher Harmonic Control, Ten Years of Aerospatial Experience, 16th ERF, Paper No. III.7.2, Sept. 19

8.1 G. Lehmann, R. Kube, Automatic Vibration at a Fourbladed Hingeless Model Rotor - A Wind Tunnel Demonstration, 14th ERF, Paper No 60, Milano, Sept. 1988

8.2 R.W. Du Val, C.Z. Gregory, N.K. Gupta, Design and Evaluation of a State Feedback Vibration Controller, AHS Northeast Region National Specialists' Meeting on Helicopter Vibration, Hartford, Connecticut, Nov. 1981

8.3 R. Kube, M. Achache, G. Niesl, W. Splettstößer, A Closed Loop Controller for BVI Impulsive Noise Reduction by Higher Harmonic Control, AHS 48th Annual Forum and Technology Display, Washington, DC, June 1992